

## ACCURACY OF OUT-OF-PLANE VORTICITY COMPONENT MEASUREMENT USING IN-PLANE VELOCITY VECTOR FIELD MEASUREMENTS

Julio Soria and Andreas Fouras  
Department of Mechanical Engineering  
Monash University  
Clayton, Victoria  
AUSTRALIA

### ABSTRACT

A study of the errors in out-of-plane vorticity calculated from in-plane velocity measurements has been undertaken. The primary factors of spatial velocity sampling separation and velocity measurement error have been investigated. The simulated velocity field of the Oseen vortex which is representative of a typical vortex structure has been used in this study. Different data quality has been considered in order to isolate the different sources of error and their effect on the accuracy of the vorticity measurement. The spatial velocity sampling separation is found to have a significant effect on accurate vorticity distribution measurements, resulting in a bias error which tends to underestimate the vorticity. The velocity measurement error results in the scatter of the vorticity measurements about the biased vorticity measurement obtained from velocity data without error.

### INTRODUCTION

Optical instantaneous in-plane velocity vector field measurement methods are beginning to become standard experimental tools in many fundamental and applied fluid mechanics investigations. A variety of methods are available. Some of these methods have evolved directly out of flow visualisation methods, e.g. streak measurement techniques (or streak photography) (Dimotakis *et al.* 1981 and Imaichi & Ohmi 1983) and particle tracking methods (Agui & Jimenez 1987), while some have their origins in solid surface motion measurement techniques, e.g. laser speckle velocimetry (LSV) (Barker & Fournay 1977 and Simpkins & Dudderar 1978). A derivative of LSV is particle image velocimetry (PIV). In PIV distinct seed particle images are photographically recorded

rather than their speckle interference pattern (Adrian 1986).

PIV is rapidly becoming the method of choice for experimental investigations which require velocity vector field data. Multi-exposed image acquisitions of flow planes with auto-spectrum/auto-correlation PIV analysis have been used for more than a decade in many fundamental fluid mechanics investigations, e.g. Simpkins & Dudderar (1978), Shepherd *et al.* (1991), Arroyo & Saviron (1992) and Wu *et al.* (1994). A more recent PIV method uses single-exposed sequential frames in conjunction with cross-correlation PIV analysis. Some examples of experimental hardware implementations and applications of cross-correlation digital PIV (DPIV) to instantaneous in-plane velocity vector field measurements in unsteady fluid flow are found in Willert & Gharib (1991), Graham & Soria (1994) and Soria (1995).

The availability of in-plane velocity vector field data permits the computation of the out-of-plane vorticity component field. The aim of this study is to investigate the accuracy of the out-of-plane vorticity component measurement derived from in-plane velocity vector field data. The emphasis being on the correct vorticity distribution and accurate peak vorticity measurement. The effect of the two primary factors: (i) spatial separation between the sampled velocity vector measurements,  $\Delta$ , and (ii) the error of the velocity vector measurements have been considered. Computer simulations have been performed to investigate the effect of these two factors on the out-of-plane vorticity component measurement.

### THE OSEEN VORTEX

The accuracy of out-of-plane vorticity measurements is examined at several levels of data quality,



i.e. from exact velocity field data to exact velocity data with superimposed random noise of a given peak amplitude to velocity data determined using cross-correlation DPIV analysis of computer generated particle image frames. The simulated axis-symmetric Oseen vortex velocity field is used as a model for a typical vorticity distribution of a vortex structure. The in-plane tangential velocity and out-of-plane vorticity component for the Oseen vortex are given in polar coordinates as

$$u_t(r) = \frac{-\Gamma}{2\pi r} \left[ 1 - \exp\left(\frac{-r^2}{4\nu t}\right) \right] \quad (1)$$

$$\omega_z(r) = \frac{-\Gamma}{4\pi\nu t} \exp\left(\frac{-r^2}{4\nu t}\right) \quad (2)$$

where  $r^2 = x^2 + y^2$  and  $x$  and  $y$  are in-plane Cartesian coordinates,  $\Gamma$  is the circulation,  $\nu$  is the kinematic viscosity and  $t$  is time. An instantaneous length scale  $L$  characterising the instantaneous size of the Oseen vortex can be defined as

$$L \equiv \sqrt{2\nu t}. \quad (3)$$

The results for two length scales  $L = 130$  *px* (*pixel*) and 280 *px* are presented here.

#### DIGITAL IMAGE FRAME GENERATION

The digital image frames used in this investigation are  $780 \times 780$  *px*<sup>2</sup>. The first frame consist of randomly positioned particle images with a Gaussian intensity distribution of typical diameter  $1.75 \pm 0.5$  *px* (i.e.  $0.005 \leq d_p/L \leq 0.015$ ). The digital image frames contain approximately 5 non-overlapping particle images per sampling window. The sampling window size was chosen to be square with  $L_x = L_y = 24$  *px*. Subsequent frames are generated by advancing the centres of the particle images in time using the Oseen velocity field with a 5th order Runge-Kutta integration scheme and 100 sub-steps over the  $\Delta t$  between the two frames. The new frame is then generated using the stored characteristic of each particle image and its new position. All digital frames have an 8 bit dynamic intensity range to simulate the dynamic range of commonly available digital cameras.

#### CROSS-CORRELATION PIV, VELOCITY INTERPOLATION AND VORTICITY CALCULATION

Cross-correlation PIV uses the normalised spatial cross-correlation function, defined as

$$\varrho(\Delta x, \Delta y) = \frac{\langle I_{s1}(i, j) I_{s2}(i - \Delta x, j - \Delta y) \rangle}{\sqrt{\langle I_{s1}^2(i, j) \rangle} \sqrt{\langle I_{s2}^2(i, j) \rangle}}, \quad (4)$$

to calculate the local velocity within a sampling window.  $I_{s1}$  and  $I_{s2}$  represent the sampling windows of size  $L_x \times L_y$  *px*<sup>2</sup> which are extracted from two sequential digital image frames.  $\langle \rangle$  represents the discrete correlation operator. The location of the

maximum in the normalised spatial cross-correlation function represents the average displacement of the particles within the sampling window. The complete velocity field is determined by sweeping the sampling window through the image frame. This type of PIV algorithm can resolve displacements of  $0.1 \pm 0.06$  *px* at the 95 % confidence level (Soria 1995). A more detailed discussion of the cross-correlation PIV technique can be found in Soria (1995) and references therein.

The out-of-plane vorticity measurement accuracy is dependent on the computational method used to determine it from the measured in-plane velocity vector field. Sinha & Kuhlman (1992) in considering this question have investigated the relative accuracy of using: (i) the adaptive Gaussian window interpolator based on the work of Agui & Jimenez (1987) with finite differencing to calculate the in-plane velocity gradients and hence, vorticity and (ii) a multi-quadratic interpolator with analytic differentiation to obtain the vorticity. Their study found that the latter method provided the most accurate estimate of the vorticity. Hence, for this study a variation of this latter method was adopted. The out-of-plane vorticity component is computed by interpolating the local in-plane velocity vector field using a  $\chi^2$  2nd order polynomial fit of the form:

$$\begin{aligned} u(x, y) &= \sum_{k=0}^8 u_k X_k(x) Y_k(y) \\ v(x, y) &= \sum_{k=0}^8 v_k X_k(x) Y_k(y), \end{aligned} \quad (5)$$

where  $X_k(x)$  and  $Y_k(y)$  are polynomial basis functions (see Soria 1995). The coefficients  $u_k$  and  $v_k$  for  $k = 0, 2, \dots, 8$ , are calculated by minimising a  $\chi^2$  merit function (see Press *et al.* 1987). Direct differentiation of the local polynomial velocity expansion given by Eq. (5) allows the calculation of the in-plane velocity gradient tensor components  $\partial u/\partial x$ ,  $\partial u/\partial y$ ,  $\partial v/\partial x$  and  $\partial v/\partial y$  and hence, the out-of-plane vorticity component:

$$\omega_z = \frac{\partial v}{\partial x} - \frac{\partial u}{\partial y} \quad (6)$$

The  $\chi^2$  interpolation process used to calculate the vorticity  $\omega_z$  uses a minimum of 12 data points.

#### RESULTS AND DISCUSSION

Figure 1 shows the effect of the spatial sampling separation of velocity data,  $\Delta$ , on the vorticity calculation. These results show that  $\Delta$  has a profound effect on accurate vorticity calculations. The exact vorticity is represented in this graph by a horizontal line crossing 0.0 on the vertical axis. The principal effect of  $\Delta$  is to bias the vorticity measurement by underestimating it over  $0 \leq r/L < 1.5$  and by slightly overestimating  $\omega_z$  for  $r/L > 1.5$ .



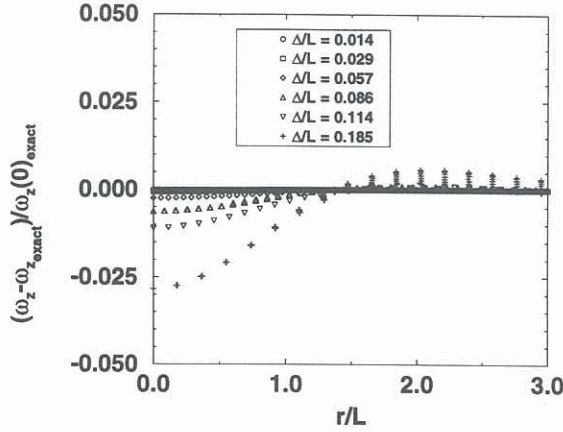
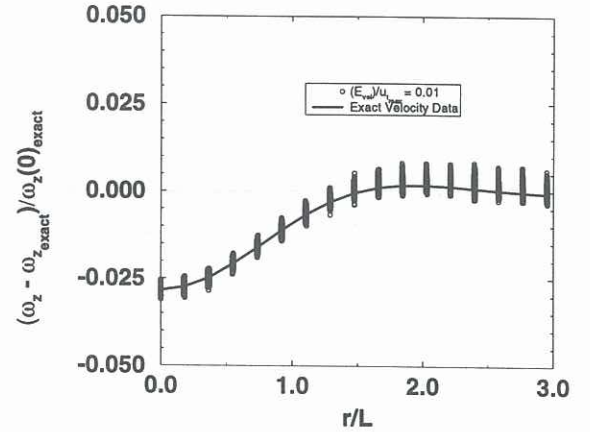


Figure 1: ERROR IN  $\omega_z$  COMPUTED USING EXACT VELOCITY DATA FOR DIFFERENT  $\Delta/L$ .

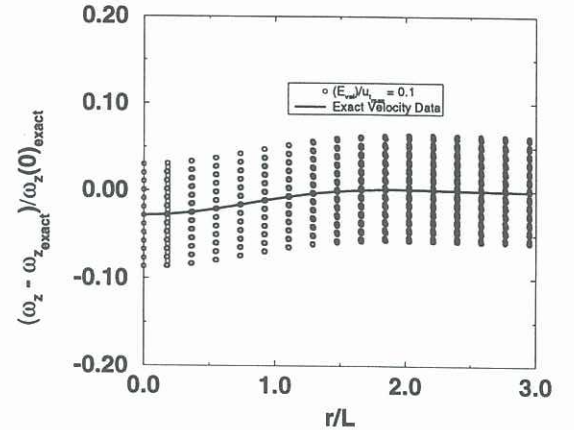
Although, the bias error for these ideal cases appears encouraging, it must be kept in mind that these cases represent a requirement for a large number of highly resolved velocity measurements across a vortex structure. For example in an ideal case with  $\Delta/L = 0.185$  at least 35 velocity measurements are required across a vortex structure to keep the maximum relative vorticity error due to this bias below 3%. This represents 1225 velocity measurements on a regular grid covering the area of a typical axis-symmetric vortex structure – a stringent requirement for many practical vorticity measurements in turbulent flows. The correlation of the  $|(\omega_z - \omega_{z\_exact})/\omega_z(0)_{exact}|$  with  $\Delta/L$  indicates that it scales linearly with  $\Delta/L$  and furthermore, that the gradient of this linear correlation is approximately 0.55.

Figures 2 (a) and (b) show the result of velocity measurement error on vorticity measurements for  $\Delta/L = 0.185$ . The simulated velocity field data in this case comprised the exact velocity with superimposed uniformly distributed random noise of a given maximum amplitude. At each  $r/L$  station a local velocity field was established with the required  $\Delta$ . Noise was then added to each velocity component prior to the vorticity calculation. The results presented in Fig. 2 represent 5000 such vorticity measurements per  $r/L$  station. The effect of velocity measurement error is clearly observable, resulting in the scatter of the vorticity measurements around the biased vorticity which was derived using exact velocity field data.

Figure 3 (a) shows that the error introduced by the DPIV analysis also results in the scatter of the vorticity measurements around the vorticity derived using exact velocity field data, with the tendency for the vorticity measurements to have the same bias due to  $\Delta$ . The bounds of the scatter of the vorticity measurements in Figure 3 (a) are similar to those in Fig. 2 (b) for simulated 10 % peak noise level. An analysis of the distribution of the error in the raw DPIV velocity data for the case shown in Figure 3 (a) revealed



(a) 1 % PEAK NOISE LEVEL



(b) 10 % PEAK NOISE LEVEL

Figure 2: ERROR IN  $\omega_z$  COMPUTED USING EXACT VELOCITY DATA WITH SUPERIMPOSED UNIFORMLY DISTRIBUTED RANDOM NOISE FOR  $\Delta/L = 0.185$ .

that this error is also of the order of 10 %. Hence, the scatter of the vorticity measurements shown in Figure 3 (a) is predominantly due to velocity measurement error.

Figure 3 (b) shows how the effect of velocity measurement error on vorticity measurement error can be reduced by calculating a  $\chi^2$  interpolated velocity field using a minimum of 9 data points from the raw DPIV velocity field prior to the vorticity calculation. The interpolated velocity field has the same  $\Delta$  as the raw DPIV velocity field data. The scatter of the vorticity measurements is smaller than the scatter observed in the vorticity derived using the raw DPIV velocity data (Fig. 3 (a)). However, the smoothing process due to the  $\chi^2$  interpolation of the DPIV velocity field introduces an additional bias error in the vorticity near the vortex core, resulting in further underestimation of the peak vorticity. It is noted that over most of the vortex domain the bias underestimation of the vorticity is still present and thus, not affected by the  $\chi^2$  interpolation process (i.e. smoothing process) of the DPIV velocity field.

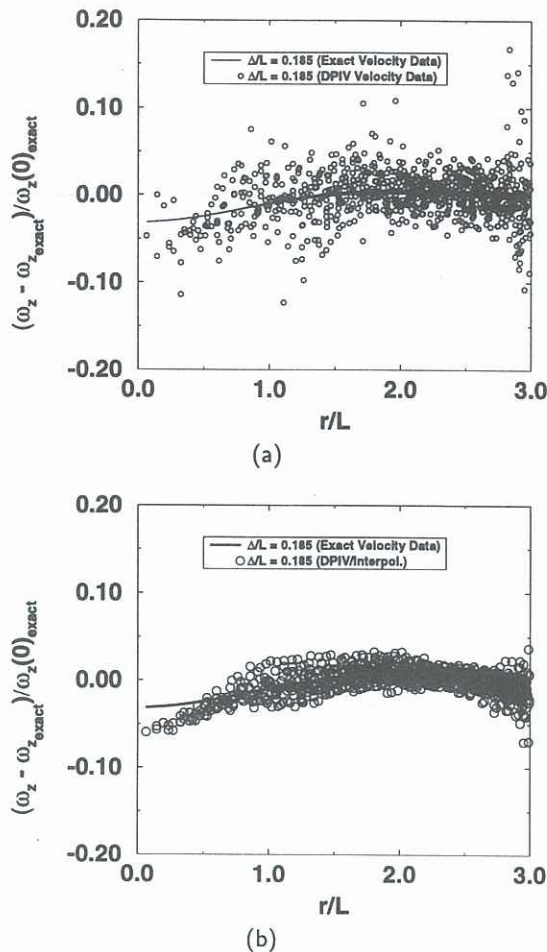


Figure 3: COMPARISON BETWEEN ERROR IN  $\omega_z$  CALCULATED: (a) DIRECTLY USING RAW DPIV DATA AND (b) USING  $\chi^2$  INTERPOLATED DPIV DATA, FOR  $\Delta/L = 0.185$ .

## CONCLUSION

This study has quantitatively shown the effects of velocity spatial sampling resolution and velocity measurement error on vorticity measurements in axis-symmetric vortex structures. The effect of the velocity spatial sampling resolution is to introduce a bias error, resulting in an underestimation of the vorticity. The maximum bias error is found to occur at the vortex core. The effect of velocity measurement error is to scatter the vorticity measurements around the corresponding biased vorticity determined using error-free velocity data. The bounds of scatter are dependent on the magnitude of the error in the velocity measurements.  $\chi^2$  interpolation of the local velocity prior to vorticity calculation reduces the vorticity scatter at the expense of additional underestimation of vorticity near the vortex core.

## REFERENCES

- Adrian, R. J. 1986 "Multi-point optical measurements of simultaneous vectors in unsteady flow - A review." *Int. J. Heat Fluid Flow* **7**, 127-145.
- Agui, J. C. & Jimenez, J. 1987 "On the performance of particle tracking." *J. Fluid Mech.* **185**, 447-468.
- Arroyo, M. P. & Saviron, J. M. 1992 "Rayleigh-Bernard convection in a small box: spatial features and thermal dependence of the velocity field." *J. Fluid Mech.* **235**, 325-348.
- Barker, D. B. & Fournay, M. E. 1977 "Measuring fluid velocities with speckle patterns." *Opt. Lett.* **1**, 135-137.
- Dimotakis, P.E., Debussy, F.D. & Koochesfahani, M.M. 1981 "Particle streak velocity field measurements in a two-dimensional mixing layer." *Phys. Fluids* **24**, 995-999.
- Graham, L.J.W. & J. Soria 1994 "A Study of an inclined cylinder wake using digital particle image velocimetry" *Proc. of 7th Int. Symp on Laser Applications in Fluid Mechanics, Lisbon, Portugal*.
- Imaichi, K. & Ohmi, K. 1983 "Numerical processing of flow-visualisation pictures - measurement of two-dimensional vortex flow." *J. Fluid Mech.* **129**, 283 - 311.
- Press, W.H., Flannery, B.P., Teukolsky, S.A. & Vetterling, W.T. 1987 *Numerical Recipes*. Cambridge University Press.
- Shepherd, R. F., LaFontaine, R. F., Welch, L. W., Soria, J. & Pearson, I. G. 1991 "Measurement of instantaneous flows using particle image velocimetry." *Second World Conf. on Exp. Heat Transfer, Fluid Mechanics and Thermodynamics, Dubrovnik, Yugoslavia*.
- Simpkins, P. G. & Dudderar, T. D. 1978 "Laser speckle measurement in transient Bernard convection." *J. Fluid Mech.* **89**, 665-671.
- Sinha, S.K. & Kuhlman, P.S. 1992 "Investigating the use of stereoscopic particle streak velocimetry for estimating the three-dimensional vorticity field." *Expt Fluids* **12**, 377-384.
- Soria, J. 1995 "An investigation of the near wake of a circular cylinder using a video-based digital cross-correlation particle image velocimetry technique." *Expt Thermal and Fluid Sci*, accepted for publication.
- Willert, C. E. & Gharib, M. 1991 "Digital particle image velocimetry." *Expt Fluids* **10**, 181-193.
- Wu, J., Sheridan, J., Soria, J. & Welsh, M. C. 1994 "An investigation of unsteady flow behind a circular cylinder using a digital PIV method." *Laser Anemometry - 1994: Advances and Applications, ASME FED-Vol 191* 167 - 172.